Citation: Cell Death and Disease (2011) 2, e145; doi:10.1038/cddis.2011.28

www.nature.com/cddis

Cell-type-specific regulation of raft-associated Akt signaling

Y Liu[1], G Yang[2], X Bu[3], G Liu[3], J Ding[3], P Li*[,1] and W Jia*[,3]

20*S*-protopanaxadiol (aPPD) is a metabolite of ginseng saponins, which is reported to be pro-apoptotic in some cells but anti-apoptotic in neuronal cells by regulating Akt signaling. Owing to its cholesterol-like structure, we hypothesized that aPPD may regulate Akt signaling by interacting with lipid rafts. Here, we compared Akt signaling in glioblastoma U87MG and neuroblastoma Neuro-2a cells treated with aPPD. aPPD did not change Akt activity in the total plasma membranes of each cell type, but drastically altered the activity of raft-associated Akt. Strikingly, Akt activity was decreased in the rafts of U87MG cells but increased in N2a cells by aPPD through regulating raft-associated dephosphorylation. The bidirectional regulation of raft-associated Akt signaling by aPPD enhanced the chemotoxicity of Paclitaxel or Vinblastine in U87MG cells but attenuated the excitotoxicity of *N*-methyl-D-aspartate in N2a cells. Our results demonstrated that the activity of raft-associated but not total membrane Akt determines its cellular functions. Lipid rafts differ in different types of cells, which allows for the possibility of cell-type-specific targeting for which aPPD might prove to be a useful agent.
Cell Death and Disease (2011) **2,** e145; doi:10.1038/cddis.2011.28; published online 14 April 2011
Subject Category: Cancer

20*S*-protopanaxadiol (aPPD) is a gastrointestinal metabolite of ginseng saponins. The latter are the main pharmacologically active components in ginseng. aPPD is an interesting compound that seems to have opposite effects on non-neuronal cells and neuronal cells. Previous studies by our group and others have shown that aPPD inhibited Akt activity and induced apoptosis in various tumor cells.[1–3] However, aPPD has also been demonstrated to protect neuronal cells against glutamate and *N*-methyl-D-aspartate (NMDA)-induced excitotoxicity[4,5] and to stimulate neuronal cell regeneration by activating the Akt pathway.[6,7] The mechanism underlying the cell-type-dependent effects of aPPD has not yet been elucidated.

The plasma membrane (PM), as a major site of Akt activation, contains multiple microdomains, and among these, a cholesterol-rich, detergent-resistant type of microdomain known as the lipid raft has been suggested as a critical platform for cell signaling.[8,9] Lipid rafts function as contributors to lateral membrane heterogeneity and are generated through lipid–lipid and specific lipid–protein interactions.[10] Owing to the long and saturated fatty acids of sphingolipids and cholesterol, lipid rafts exist in the liquid-ordered phase. In contrast, other PM compartments occur in the liquid-disordered phase because they are composed of phospholipids with short and unsaturated fatty acids.[11] Cholesterol is believed to serve as a spacer between the hydrocarbon chains of sphiongolipids and to function as a dynamic glue that keeps the raft assembly together.[12]

Akt signaling in PM microdomains has only recently been examined as an important oncogenic pathway.[13–15] The binding of growth factors to their receptor tyrosine kinases stimulates the phosphorylation of phosphatidylinositol 3-kinase (PI3K) comprised of P85 and P110 subunits, which localize to lipid rafts. PI3K converts phosphatidylinositol-4,5-bisphosphate (PI(4,5)P2) to phosphotidylinositol-3,4,5-trisphosphate (PI(3,4,5)P3), whereas phosphatase and tensin homolog deleted on chromosome 10 reverses this reaction. Akt translocates to the PM and interacts with PI (3,4,5)P3 via its PH domain and is, respectively, phosphorylated at two residues (Thr308 and Ser473) by phosphoinositide-dependent kinase (PDK) and various raft-associated kinases, including mTORC2 and integrin-linked kinase (ILK).[16,17] One of the first targets of Akt shown to have direct implications in the regulation of cell survival is a member of the proapoptotic Bcl-2-family and is known as Bcl-2-associated death (BAD). It is attached to lipid rafts in proliferating cells, although associated to mitochondria in apoptotic cells.[12,18] Once phosphorylated, the phosphoserine residues (Ser136 and Ser112) of BAD form affinity-binding sites for 14-3-3 molecules, thus localizing phosphorylated BAD to the cytosol

[1]Department of Pathology, School of Preclinical Medicine, Beijing University of Chinese Medicine, 11 Bei San Huan Dong Road, Chaoyang District, Beijing 100029, China; [2]Department of Neuroscience, College of Interdisciplinary Studies and Brain Research Centre, University of British Columbia, 2211 Wesbrook Mall, Vancouver, British Columbia V6T 2B5, Canada and [3]Department of Surgery and Brain Research Centre, University of British Columbia, F233-2211 Wesbrook Mall, Vancouver, British Columbia V6T 2B5, Canada
*Corresponding authors: P Li, Department of Pathology, School of Preclinical Medicine, 5 Hai Yun Cang, Dongzhimen Hospital affiliated with Beijing University of Chinese Medicine, Dongcheng District, Beijing 100700, China. Tel: +86 10 84013206; Fax: +86 10 64010817; E-mail: Lptao@263.net or W Jia, Department of Surgery and Brain Research Centre, University of British Columbia, F233-2211 Wesbrook Mall, Vancouver, British Columbia, Canada V6T 2B5. Tel: +604 822 0728; Fax: +604 322 0640; E-mail: wjia@interchange.ubc.ca
Keywords: 20*S*-protopanaxadiol; Akt; apoptosis; lipid rafts
Abbreviations: aPPD, 20S-protopanaxadiol; BAD, Bcl-2-associated death promoter; MβCD, methyl-β-cyclodextrin; NMDA, *N*-methyl-D-aspartate; PHLPP, PH domain leucine-rich repeat phosphatase; PM, plasma membrane; TAXOL, Paclitaxel
Received 04.1.11; revised 28.2.11; accepted 08.3.11; Edited by V De Laurenzi

and effectively neutralizing its pro-apoptotic activity.[19,20] Recent studies indicated that raft-associated Akt could be an important determinant of oncogenicity.[21,22] Studies of small-cell lung cancer cells showed that specific PI3K isoforms reside in lipid rafts and that disruption of membrane rafts by methyl-β-cyclodextrin (MβCD) inhibits PI3K-mediated Akt activity.[23] Live-cell fluorescence imaging has shown that raft Akt is activated faster and more potently than non-raft Akt, presumably because of compartmentalization of various components of the signaling pathway, including the receptors, PI3K and Akt itself.[22]

Given their saponin-like structure, ginsenosides are well known for their ability to increase the fluidity of cellular membranes.[11,24] As the structure of aPPD highly resembles that of cholesterol, we hypothesized that this compound may interfere with lipid rafts and alter lateral movement of raft resident proteins. We further speculated that different types of cells might differ in the resident proteins of their lipid rafts, which may explain the abovementioned contrast in the effects of aPPD on neurons *versus* non-neuronal cells. To test the above hypothesis, we used the glioma cell line U87MG and the neuroblastoma cell N2a for our investigation. Although both the cells have a nerve tissue origin, they differ in that U87MG is derived from glial cells and N2a is a neuronal cell type.[25,26] Following treatment of both cell types with aPPD, we investigated the Akt signaling pathway in the lipid rafts and consequently, their cellular response to chemotherapeutic and excitotoxic agents. Our results showed that aPPD altered raft-associated Akt activity differently in the two cell lines but not in the total PM. Moreover, the cellular outcomes to a toxic stimulus were opposite, indicating that the pharmacological effects of this compound can be completely cell-type-specific because of differences in its effect on the raft-associated cell signaling of different cells.

Results

aPPD affects lipid rafts differently from MβCD and these effects are cell-type dependent. To demonstrate the differential effects of aPPD on lipid rafts in the two cell lines, we looked at changes in cholesterol concentrations of various PM fractions of U87MG and N2a cells treated with aPPD or MβCD. The latter is a well-known lipid raft disruptor, which functions by depleting membrane cholesterol.[11,27] To examine whether aPPD is cytotoxic to the cells, cell mortality were measured with different concentrations of aPPD at different time points. Although treatment with 10 μM aPPD had no effect on cell mortality at 4 h for both cells 5.20 $\pm$ 2.45%, $P = 0.196$) for U87MG and 3.76 $\pm$ 5.97%, $P = 0.276$) for N2a cells), the mortality increased slightly, but not statistically significant by 24 h (12.64 $\pm$ 13.57%, $P = 0.089$ in U87MG cells and 11.30 $\pm$ 10.41% in N2a cells, $P = 0.059$). Significant cell death was observed at 24 h in cells treated with 20 μM aPPD, especially not only for U87MG (42.7 $\pm$ 14.78%, $P = 0.002$) but also for N2a to a less degree (23.12 $\pm$ 5.39, $P = 0.002$). Thus, 10 μM aPPD was used in the following experiments. Cellular membranes were separated at 4 h after treating with 10 μM aPPD through ultracentrifugation into 12 fractions (Figure 1b). The lipid rafts were mainly located in fraction 5 as demonstrated by western blots of flotillin-1, a lipid raft marker (Figure 1c). As expected, the maximum cholesterol content was also found in fraction 5 of both untreated U87MG and N2a cells (Figures 2a and b), further confirming enrichment of the lipid rafts in this fraction. Treatment with 10 mM MβCD completely diminished the cloudy appearance of fraction 5 of membrane proteins of both cell types (Figure 2c) and significantly reduced the levels of total cholesterol in this fraction (Figures 2a and b), suggesting a complete disruption of the lipid rafts of both cell types by this agent. Treating cells of both lines with aPPD also diminished the cloudy appearance of fraction 5 (Figure 2d). Surprisingly, however, there was no change in cholesterol levels in this fraction (Figures 2a and b), indicating that, unlike MβCD, aPPD does not cause any depletion of membrane cholesterol. Furthermore, levels of flotillin-1 protein in both U87MG and N2a cells decreased in fraction 5 after MβCD treatment (Figure 3a). However, treatment with aPPD reduced the flotillin-1 concentration in U87MG cells only. Instead, aPPD treatment upregulated the flotillin-1 level in the rafts of N2a cells to 142.91 $\pm$ 10.71% of the control, as shown in Figure 3b. Taken together, these data suggested that aPPD can interfere with lipid rafts but not by the same mechanism used in the case of MβCD. Furthermore, aPPD can have an opposite effect on raft resident protein flotillin-1, depending on the cell type.

aPPD alters raft-associated Akt phosphorylation without changing the total membrane Akt level. We then asked whether aPPD altered levels of Akt and its phosphorylation status in the cellular membrane of the two types of cells. Western blots of total Akt and its two phosphorylation residues, Thr308 and Ser473, were performed with total membrane proteins of U87MG and N2a cells treated with aPPD. Figures 4a and b show that there were no significant changes in Akt or its state of phosphorylation in the PM of each type of aPPD-treated cells.

Interestingly, Akt and its phosphorylation state were totally different in the lipid rafts isolated from the two different types of aPPD-treated cells. As shown in Figures 4c and d, although aPPD did not significantly change the total level of Akt in the lipid rafts of the two cell types, phosphorylation at Thr308 and Ser473 was significantly reduced in U87MG cells but increased in N2a, indicating that aPPD may inhibit raft-associated Akt activity in U87MG cells but stimulate this activity in N2a cell.

aPPD regulates Akt activity in lipid rafts by altering levels of raft-associated phosphatases. To determine how aPPD selectively activates raft-associated Akt activity in N2a cells but inhibits it in U87MG cells, we measured levels of PI3K, PDK and ILK in the lipid rafts, which are known as upstream kinases that regulate the phosphorylation of Akt.[17] As shown in Figure 5a, we noted no significant changes in PI3K, including activity involving the regulatory subunit P85 and the catalytic subunit P110α, after aPPD treatment of either U87MG or N2a cells. We further investigated whether raft levels of PDK1 and ILK, which, respectively, phosphorylate Thr308 and Ser473 of Akt, were

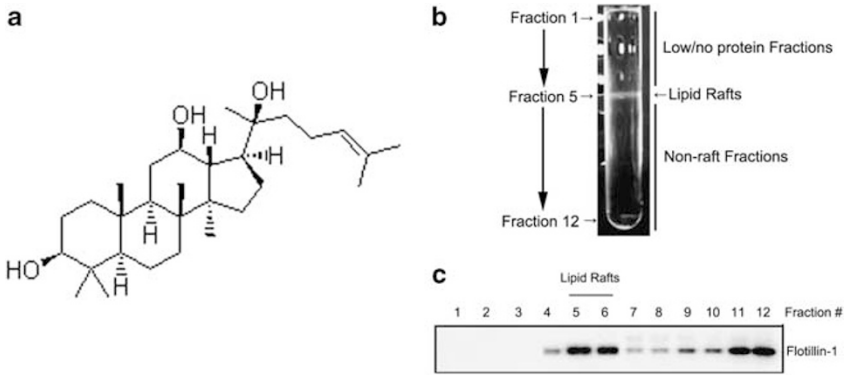

Figure 1 Isolation and identification of lipid rafts. (**a**) The chemical structure of 20*S*-Protopanaxadiol (aPPD). (**b**) Membrane preparations after centrifugation to isolate lipid rafts as described in Materials and methods. Lipid rafts were mainly in fraction 5 appearing as an opaque band. (**c**) Proteins in each fraction shown in (**b**) were analyzed by SDS-PAGE and blotted with flotillin-1 antibody. As a lipid raft resident protein, flotillin-1 was mainly present in fraction 5 (sometimes also in 6). All results are representative of at least three independent experiments

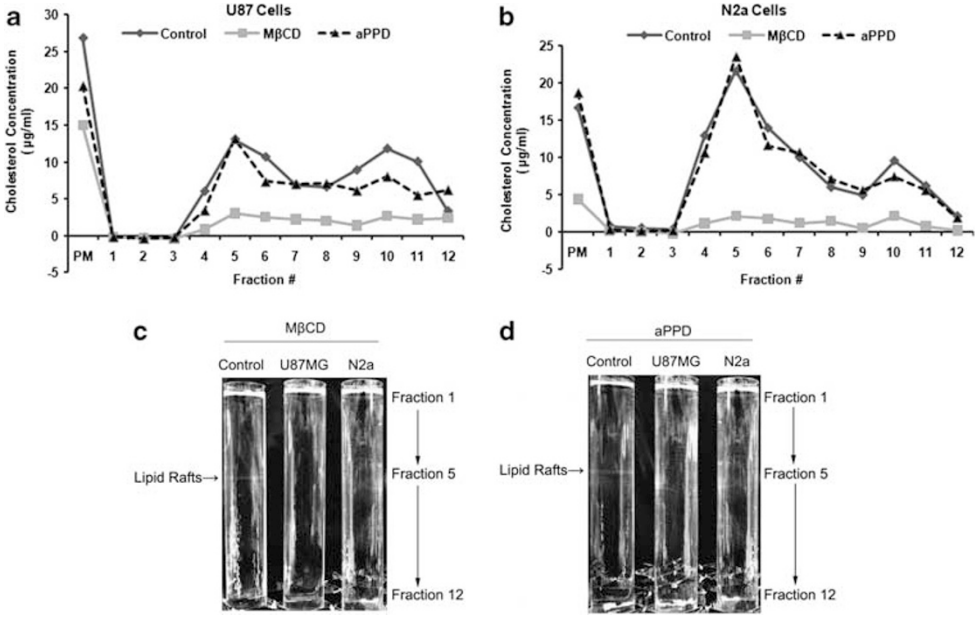

Figure 2 aPPD does not deplete cholesterol in the membrane. (**a**) The cholesterol concentrations in the PM and each fraction of U87MG cells measured with an Amplex Red cholesterol assay kit. (**b**) The cholesterol concentrations in the PM and each fraction of N2a cells. The highest level of cholesterol was detected in fraction 5 in both cell lines. (**c** and **d**) Cellular membrane samples of 10 mM MβCD- or 10 μM aPPD-treated U87MG and N2a cells collected by centrifugation. Although both MβCD and aPPD caused a disappearance of the opaque band, only MβCD and not aPPD depleted cholesterol (**a** and **b**). $^{*}P<0.05$, $^{**}P<0.001$ compared with the control, *t*-test ($n=3$ independent experiments)

affected by the aPPD treatment. Figure 5b shows that the amount of PDK1 did not change significantly in each type of aPPD-treated cell. However, the amount of ILK1 in the lipid rafts of N2a cells increased significantly, whereas it decreased in those of U87MG. Finally, we measured levels of two major phosphatases, PH domain leucine-rich repeat phosphatase 1 and 2 (PHLPP1 and 2), that are responsible for Akt dephosphorylation.[28–33] Our results (Figure 5c) showed that treatment with aPPD caused significant changes in both PHLPP1 and PHLPP2 in lipid rafts. Strikingly, the level of PHLPP1 and PHLPP2 in the rafts increased by 56.31 ± 5.12 and 82.97 ± 5.02%, respectively, in U87MG cells but decreased by 30.38 ± 3.94 and 30.22 ± 8.31% in N2a cells.

Bidirectional regulation of Akt functions of glioma cells *versus* neuronal cells. To examine whether the contrasting effects of aPPD on raft-associated Akt in the two types of cells correlate with a difference in their respective pharmacological responses, we measured cell viability under toxic insult with or without aPPD. U87MG cells were treated with different concentrations of Paclitaxel (TAXOL) (Bristol-Myers Squibb, Toronto, ON, Canada), or Vinblastine and N2a cells were treated with NMDA. Both cells were co-treated with 10 μM aPPD. Remarkably enhanced toxicity was evident in U87MG cells co-treated with aPPD and TAXOL or Vinblastine (Figures 6a and b). In contrast, aPPD strongly protected N2a cells from NMDA-induced excitotoxicity (Figure 6c).

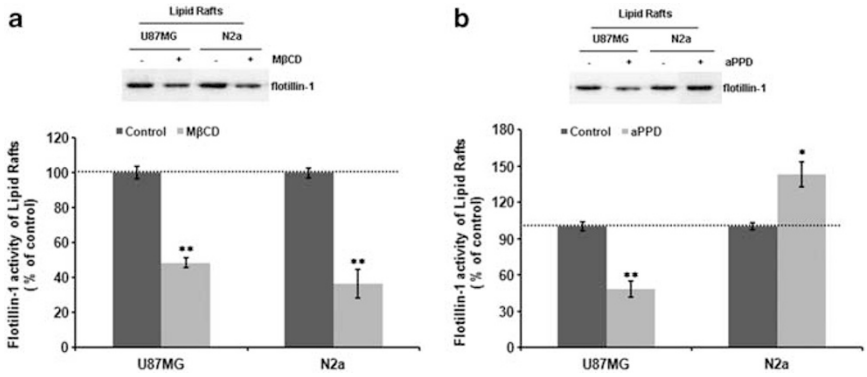

Figure 3 Levels of flotillin-1 in the lipid rafts of both U87MG and N2a cells treated with either MβCD (**a**) or aPPD (**b**). *$P<0.05$, **$P<0.001$ compared with the control, *t*-test ($n=3$ independent experiments)

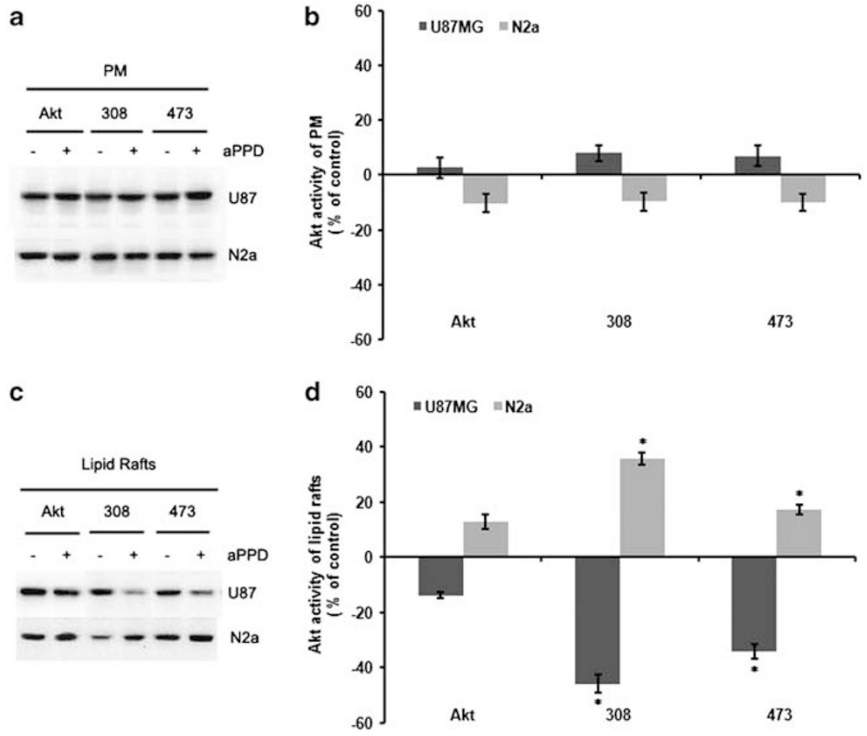

Figure 4 Effect of aPPD on Akt activity in the cellular membrane. aPPD had no effect on the Akt concentration or its phosphorylation state in either U87MG or N2a cells (**a** and **b**). aPPD regulates Akt phosphorylation in the lipid rafts of U87MG and N2a cells in an opposite manner (**c** and **d**). *$P<0.05$ compared with the control, *t*-test ($n=3$ independent experiments)

Finally, we asked whether the above difference in the pharmacological effects of aPPD could be attributed to its different effects on the Akt pathway in the lipid rafts of the two cell lines under the toxic insults. We compared levels of raft-associated Akt and phosphorylated Akt, as well as BAD. The latter is a downstream target of Akt, and BAD phosphorylation is an important anti-apoptotic mechanism of Akt signaling. Neither TAXOL nor Vinblastine significantly altered Akt activity in the lipid rafts of U87MG cells (Figures 7a and c). In addition, both chemotherapeutic agents significantly reduced the total levels of BAD in the lipid rafts of U87MG cells but did not affect their phosphorylation state (Figures 7b and d). On the other hand, NMDA significantly reduced phosphorylation of Akt in the lipid rafts of N2a cells and consequently, the phosphorylation of raft-associated BAD was also reduced (Figures 7e and f). As expected, aPPD drastically suppressed Akt phosphorylation in the lipid rafts in TAXOL- or Vinblastine-treated U87MG cells. Levels of BAD phosphorylation were also significantly reduced (Figures 7a-d). In contrast, aPPD restored the phosphorylation status of Akt and BAD in the lipid rafts of NMDA-treated N2a cells (Figures 7e and f). Thus, these results confirm that aPPD exerts opposite pharmacological effects on these different cell types and this cell-type-specific, bidirectional phenomenon can be attributed to the cell-type-specific difference in the activity of aPPD in raft-associated Akt signaling.

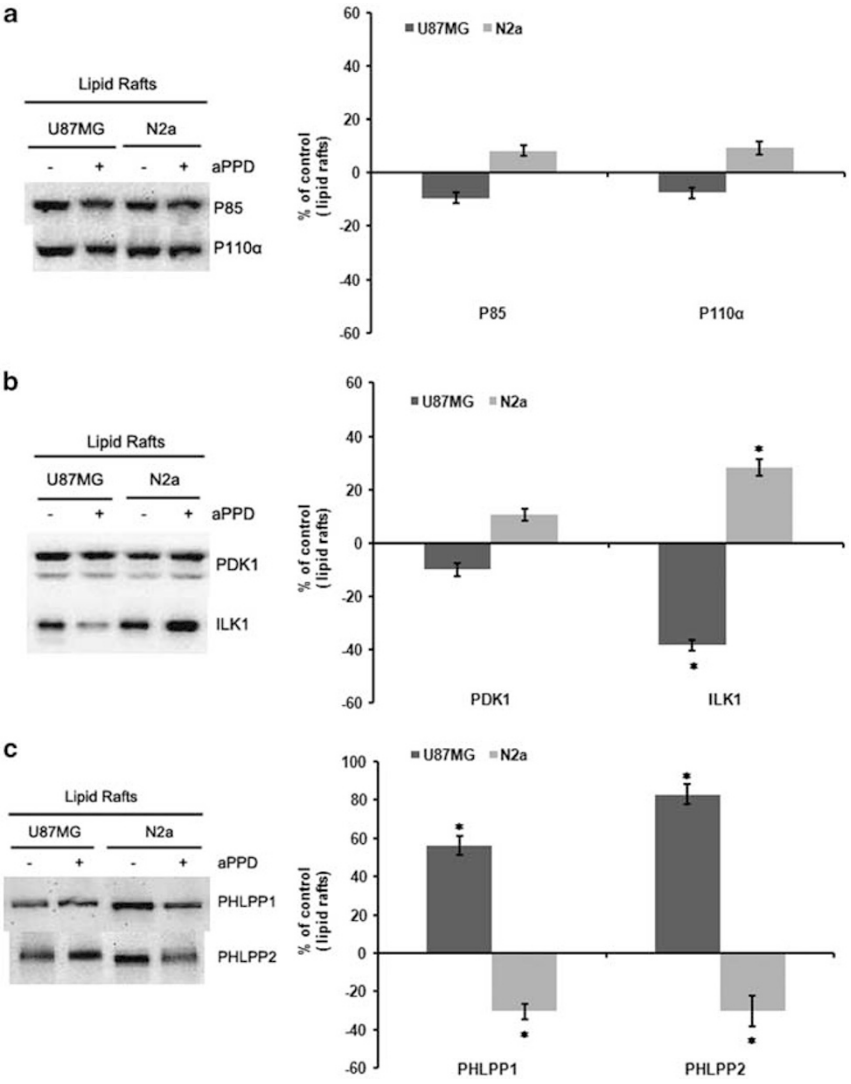

Figure 5 Effects of aPPD on Akt regulators in lipid rafts. (**a**) There were no significant changes in levels of P85 and P110α of PI3K after treatment with aPPD in either U87MG cells or N2a cells. (**b**) The amount of PDK1 did not change significantly in aPPD-treated cells of each cell line. However, the amount of ILK1 in the lipid rafts significantly increased in N2a cells and decreased in U87MG cells. (**c**) The levels of PHLPP1 and PHLPP2 in the rafts significantly increased in U87MG cells but, respectively, decreased in N2a cells. $^*P<0.05$ compared with the control, *t*-test ($n=4$ independent experiments)

aPPD inhibits glioma cell migration. Raft-associated Akt signaling pathway is known to regulate cell invasion and motility.[34] Thus, *in vitro* scratch assay[35] was performed to measure 24-h cell migration rates of both U87MG and N2a cells treated with aPPD. Figure 8 showed that treatment with aPPD significantly inhibited cell migration in U87MG cells ($53.2\pm20.1\%$ of control, $P=0.0002$), but had much less effect on N2a cells ($82.4\pm20.8\%$, $P=0.166$).

Discussion

The above results clearly show that (1) aPPD is highly effective in interfering with the protein composition of the lipid rafts without altering the level of cholesterol; (2) the effects of aPPD on the raft resident proteins are highly cell-type dependent; (3) aPPD suppresses the activity of the Akt pathway in the lipid rafts of glioma cells but increases it in neuronal cells without affecting the Akt activity in the total PM of both types of cells; (4) the raft-associated Akt activity is regulated by aPPD by altering the levels of phosphatases in the raft; (5) the difference in the effect of aPPD on the activity of the raft-associated Akt pathway results in inhibition on cell migration and enhanced cytotoxicity with TAXOL or Vinblastine in U87MG cells, but attenuated excitotoxity with NMDA in N2a cells; Our study demonstrates that the final metabolite of protopanaxadiol ginsenosides, aPPD, is a highly effective raft disruptor. Unlike MβCD, aPPD alters the contents of resident proteins in the lipid rafts without changing the levels of cholesterol. Rh2, a glycosylated form of protopanaxadiol has also been shown to influence the lateral movement of Fas between raft and non-raft microdomains of the cellular membrane.[11] As aPPD is structurally more similar to cholesterol, it would not be surprising if it functions as a stronger raft disruptor through intercalating itself into the lipid

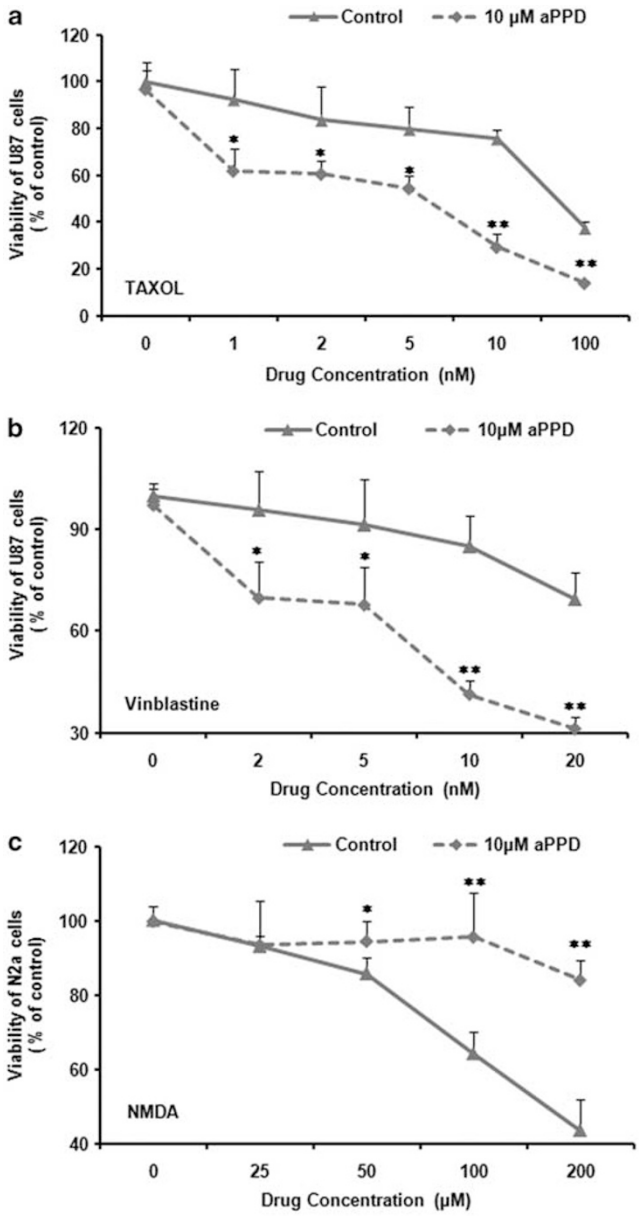

Figure 6 aPPD enhanced the cytotoxic effect of chemotherapeutic agents in glioma cells and attenuated the cytotoxic effect in NMDA-treated neuronal cells. (**a** and **b**) U87MG cells were incubated with or without 10 μM aPPD in the presence of different concentrations of either Paclitaxol (TAXOL) or Vinblastine. (**c**) aPPD remarkably reduced NMDA-induced neuroexcitotoxicity in N2a cells. $^{*}P<0.05$, $^{**}P<0.001$ compared with the control, *t*-test ($n=3$ independent experiments)

rafts to cause changes in the microenvironment of the membrane, which in turn results in an alteration of the protein composition of the lipid rafts. It remains to be determined whether aPPD alters raft resident proteins by causing a general alteration in the fluidity of the membrane, similar to other cholesterol derivatives,[36] or whether the compound directly interacts with specific proteins in the lipid rafts to modulate their activity. It is worth noting that even though aPPD does not change the cholesterol level in the lipid rafts, it caused the opacity of the lipid raft fraction to disappear, as did MβCD (Figure 2). As the opacity might indicate the presence of a specific form of complex containing insoluble proteins and lipid, its aPPD-induced disappearance clearly suggests that the compound can alter the physical state of the proteins in the lipid rafts.

The most striking finding of the present investigation is that aPPD regulates the raft-associated Akt pathway of glioma cells and neuronal cells in an opposite manner. aPPD downregulates Akt phosphorylation in U87MG cells but upregulates the phosphorylation in N2a cells. Results showed that this bidirectional regulation of the activity of raft-associated Akt by aPPD was not due to changes in the activity of PI3K or PDK1 in the rafts (Figure 5). The latter is responsible for phosphorylation at Thr308, which is thought to be essential for Akt activation.[37] As aPPD altered the Akt phosphorylation status with no change in PI3K or PDK1, it is more likely that Akt activity was regulated by changes in raft-associated phosphatases. Indeed, cell-type-specific alteration in raft-associated PHLPPs was observed in aPPD-treated cells. Both phosphatases are known for their role in attenuating the total level of Akt hydrophobic motif phosphorylation and cell survival.[28] There is no obvious explanation for the contrasting effects of aPPD on the two cell lines with respect to Akt signaling in their lipid rafts. It has been reported that PHLPP1 might be associated with Akt2 and Akt3, whereas PHLPP2 might be with Akt1 and Akt3.[33] It remains to be studied whether differential distribution of the Akt isoforms and their PHLPPs has any role in their functions in the lipid rafts of different cell types. Alternatively, it is also possible that cells may differ in the respective structures of lipid rafts such as those reflecting the composition of resident proteins, and that these differences could be elucidated with lipid raft proteomic analysis.[38]

The above bidirectional regulation of raft-associated Akt signaling by aPPD is highly consistent with the contrasting pharmacological activity of this compound in U87MG cells and N2a cells when co-stimulated with toxic insult (Figure 6). It is interesting that, in U87MG cells, both TAXOL and Vinblastine significantly reduced the total amount of raft-associated BAD, the phosphorylating target of Akt, without changing the amount of phosphorylated BAD in the lipid rafts. As there was no significant difference in Akt activity in the rafts of drug-treated cells, it appears that the chemotherapeutic agents increased the ratio of phosphorylated BAD to non-phosphorylated BAD in the lipid rafts by removal of the latter from these structures. Interestingly, in N2a cells, NMDA inhibited phosphorylation of raft-associated Akt and BAD without changing the total amounts of these proteins in the lipid rafts. Finally, aPPD enhanced chemotoxicity in U87MG cells and protected N2a cells from NMDA-induced excitotoxicity. These bidirectional effects were in agreement with the changes observed in Akt activity as well as in its downstream target BAD in the lipid rafts of the two cell types, which may directly correlate with the cell-type-dependent pro-apoptotic or anti-apoptotic effect of aPPD. More importantly, the fact that aPPD's pharmacological functions correlate with activity of raft-associated Akt but not that in the total PM further emphasizes the notion that only raft-associated Akt determines the functions of its signaling.

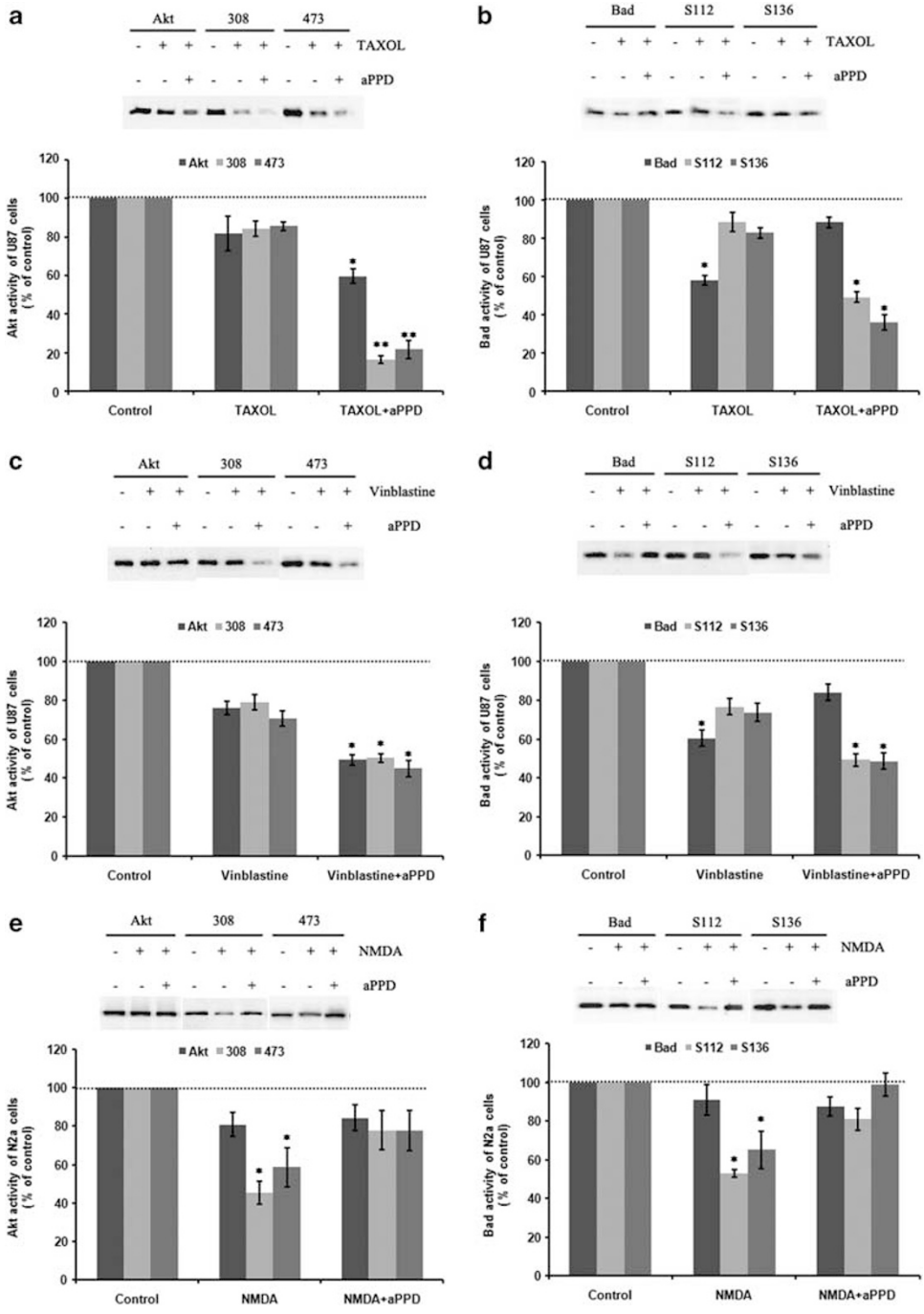

Figure 7 Akt signaling in lipid rafts of U87MG and N2a cells treated with chemotherapeutics and NMDA with and without aPPD. Total Akt and Akt phosphorylation in the lipid rafts were inhibited by aPPD in U87MG cells treated with TAXOL or Vinblastine (**a** and **c**). Phosphorylation of BAD in the lipid rafts was also reduced by aPPD (**b** and **d**). aPPD restored phosphorylation of Akt and BAD in the lipid rafts of N2a cells treated with NMDA (**e** and **f**). $^{*}P<0.05$, $^{**}P<0.001$ compared with the control, *t*-test ($n=3$ independent experiments)

In the present study, we show that only phosphorylation of raft-associated Akt determines the activity and direction of Akt signaling, as aPPD has no effect on Akt phosphorylation in the total PM of the two cell types. This underlines the importance of focusing on membrane microdomains instead of the global cellular membrane when the functions of signaling proteins are studied. Our results are the first to clearly demonstrate that cells can be differentially targeted according to differences in the structures of their membrane microdomains, and aPPD was used here as the first agent to be applied for this purpose.

Materials and Methods

Materials. aPPD was provided by Shanghai Innovative Research Centre of Traditional Chinese Medicine (Shanghai, China). The compound was 97.9% pure as measured by HPLC analysis. Antibodies to phosphor-Akt (Ser^{473}), phosphor-Akt

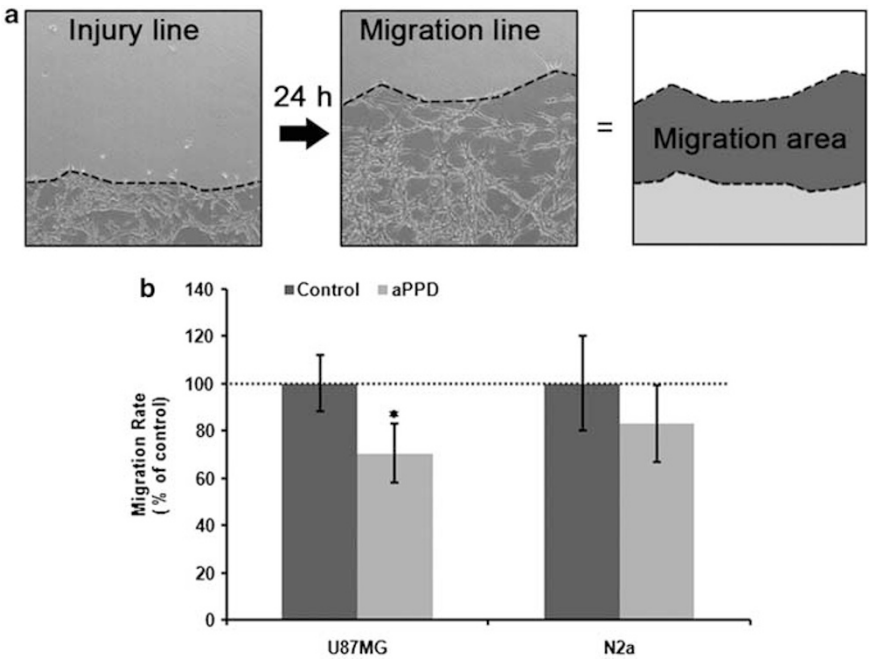

Figure 8 Effects of aPPD on cell migration of U87MG and N2a cells. (**a**) Migration of cells in culture dishes. The edges (dotted lines) of cultured U87MG cells at 0 and 24 h after scratch were shown as the injury line and the migration line, respectively. The migration area was calculated as regions between the injury and migration lines. (**b**) Quantification of the cell migration rate. The migration rate of U87MG cells was effectively reduced with the treatment of aPPD in U87MG but not N2a cells. The data were the averages of two repeated experiments with quadruplets for each time, $^*P<0.05$ compared to the control

(Thr^{308}), Akt (pan), PI3 Kinase p85, PI3 Kinase p110α, ILK1, phosphor-PDK1 (Ser^{241}), BAD, phosphor-BAD (Ser^{112}) and phosphor-BAD (Ser^{136}) were purchased from Cell Signalling Technology, Inc. (Mississauga, Ontario, Canada). Flotillin-1 antibody was purchased from Abcam, Inc. (Cambridge, MA, USA). PHLPP1 and PHLPP2 antibodies were purchased from Bethyl Laboratories, Inc. (Montgomery, TX, USA). HRP-conjugated anti-rabbit and anti-mouse IgG were purchased from Perkin-Elmer Life Sciences (Boston, MA, USA). Protease inhibitor cocktails were obtained from Roche Molecular Biochemicals (Mannheim, Germany). A modified DC protein assay kit and nitrocellulose membranes were purchased from BIO-RAD (Hercules, CA). MβCD, Vinblastine, NMDA, media (Dulbecco's modified Eagle's medium, DMEM), thiazolyl blue tetrazolium bromide (MTT) and other chemicals were purchased from Sigma (St. Louis, MO, USA). Paclitaxel was purchased from the pharmacy of the British Columbia Cancer Agency (Vancouver, BC, Canada). U87MG cells and N2a cells were purchased from American Type Culture Collection (ATCC) (Manassas, VA, USA). Phosphate-buffered saline (PBS), cell culture supplements (fetal bovine serum (FBS) and antibiotics were obtained from GIBCO BRL (Gaithersburg, MD, USA).

Cell cultures and treatments. Human U87MG and N2a cells were cultured in DMEM supplemented with 10% FBS, 100 U/ml penicillin and 100 μg/ml streptomycin, at 37°C in a humidified atmosphere containing 5% CO_2 and fed every 2–3 days. A stock solution of 50 mM aPPD was prepared in 100% ethanol and diluted to proper concentrations in DMEM immediately before each experiment. Drug-treatment cells were pretreated with DMEM for 4 h at 37°C, followed by the addition of 10 mM MβCD or 10 μM aPPD for 1 h.

Lipid raft isolation. Cells in five 100-mm dishes were mixed with 3 ml of lysis buffer per dish (150 mM NaCl, 20 mM Na_2HPO_4, 2 mM NaH_2PO_4, 20% (v/v) glycerol, 2 mM sodium orthovanadate with protease inhibitors, pH 7.4) and homogenized 30 times with a tight Dounce homogenizer (Sigma). Samples were further disrupted by intermittent sonication (six 30-s pulses with a 1 min cooling period between) and then centrifuged at 10 K r.p.m. (Beckman-Coulter Optima L-90K ultracentrifuge with an SW55Ti rotor, Mississauga, ON, Canada) for 11 min at 4°C to separate cell debris and nuclear materials. The supernatant was then centrifuged at 32.5 K r.p.m. (SW55Ti rotor) for 90 min at 4°C to pellet the PM. The PM was suspended and solubilized in 2 ml solubilizing buffer containing 0.5% v/v Triton X-100 in Mes-buffered saline (MBS: 25 mM Mes, pH 6.5/0.15 M NaCl), protease inhibitors and 2 mM sodium orthovanadate for 15 min on ice. Then, 2 ml of solubilized PM were further diluted with an equal volume of 80% sucrose in MBS and loaded on the bottom of a 13 ml ultracentrifuge tube overlaid with 4 ml of 30% sucrose/MBS. Finally, 4 ml of a 5% sucrose/MBS solution were added as the top layer of the gradient. The gradient was centrifugated at 31 K r.p.m. (SW41Ti rotor) for 16 h at 4°C to isolate the lipid raft and non-raft compartments. The gradient was then fractionated into 12 fractions.[39]

Western blotting. The protein concentration was measured using a modified DC protein assay. An equal volume of fraction (10 μl/lane) from each sample was separated on a polyacrylamide gel. For immunoblotting, the proteins were transferred onto nitrocellulose membranes using a wet transfer system (BIO-RAD). The membranes were blocked with 5% non-fat milk (BIO-RAD) for 1 h at room temperature and probed with primary antibodies at 4°C overnight. The membranes were then washed three times with Tris-buffered saline with 0.05% Tween 20 (TBST) and incubated with HRP-conjugated anti-rabbit or goat IgG (1 : 5000) for 1 h at room temperature. Signals were detected using enhanced chemiluminescence (Perkin-Elmer Life Sciences) and band intensities were quantified using Image J software (NIH, Bethesda, MD, USA).

Cholesterol measurement. Fifty microliters of each fraction were analyzed with an Amplex Red cholesterol assay kit (Molecular Probes, Eugene, OR, USA) according to the manufacturer's protocol.

MTT assay. For cell viability, cells were seeded in 96-well plates at a density of 2.5×10^4/well, 1 day before experiments. Cultures were then incubated with DMEM containing TAXOL, Vinblastine or NMDA, with or without aPPD (10 μM) for 24 h at 37°C. At the end of each time point, the culture medium was removed and 50 μl of MTT (0.5 mg/ml in serum-free medium) were added to each well. Following incubation at 37°C for 4 h, 100 μl of lysis buffer (50v/v *N,N*-dimethylformamide (Sigma), 20% SDS (BIO-RAD) and 0.4% (v/v) glacial acetic acid in distilled water (pH 4.8)) were added and the plates were incubated overnight in a humidified atmosphere (37°C with 5% CO_2). The optical density of each well was determined with a microplate reader (BIO-TEK, Winooski, VT, USA) at 595 nm.

Cell migration assay. U87MG or N2a cells were cultured in six-well culture dishes to 70–90% confluence, followed by scratch with 1 ml sterilized pipette tips. After washing with pre-warmed PBS, cells were cultured in serum-free DMEM for 24 h. Images were taken at 0 and 24 h after scratch by Zeiss Axiovert 200 microscope (Zeiss, Toronto, ON, Canada) with $\times 5$ (for U87MG cells) or $\times 10$ (for N2a cells) objectives. Images of same spots taken at 0 and 24 h were overlaid and adjusted with Photoshop CS4 software (Adobe, Ottawa, ON, Canada). The edge of cultured cells was marked by linking cell bodies of furthest, but continually, related cells from unscratched regions. The edge at 0 and 24 h were defined as the injury line and migration line, respectively. The area between injury and migration lines was considered as the migration area and was subject to quantification.[40] Areas of migration on images were measured with ImageJ.

Statistical analysis. Data were obtained from at least two independent experiments, each performed at least in triplicate. Data were expressed as means $\pm$ S.E. and analyzed for statistical significance by a two-tailed Student's *t*-test. Differences with *P*-values <0.05 were regarded as statistically significant and are indicated by an asterisk (*) in the figures.

Conflict of Interest

The authors declare no conflict of interest.

Acknowledgements. We thank Shanghai Innovative Research Centre of Traditional Chinese Medicine for providing the purified aPPD compound. We appreciate Changiz Taghibiglou for his helpful suggestions on the protocol used for isolating the lipid rafts. This study was supported by grants from the Canadian Institute of Health Research awarded to W Jia, from the China National Science & Technology Major Project (Grant 2009ZX09502-014) for Pengtao Li and from the China Scholarship Fund for Yuan Liu.

1. Jeong A, Lee HJ, Jeong SJ, Lee EO, Bae H, Kim SH. Compound K inhibits basic fibroblast growth factor-induced angiogenesis via regulation of p38 mitogen activated protein kinase and AKT in human umbilical vein endothelial cells. *Biol Pharm Bull* 2010; **33**: 945–950.
2. Liu GY, Bu X, Yan H, Jia WW. 20S-protopanaxadiol-induced programmed cell death in glioma cells through caspase-dependent and -independent pathways. *J Nat Prod* 2007; **70**: 259–264.
3. Yu Y, Zhou Q, Hang Y, Bu X, Jia W. Antiestrogenic effect of 20S-protopanaxadiol and its synergy with tamoxifen on breast cancer cells. *Cancer* 2007; **109**: 2374–2382.
4. Bao HY, Zhang J, Yeo SJ, Myung CS, Kim HM, Kim JM *et al.* Memory enhancing and neuroprotective effects of selected ginsenosides. *Arch Pharm Res* 2005; **28**: 335–342.
5. Kang SY, Kim YC. Decursinol and decursin protect primary cultured rat cortical cells from glutamate-induced neurotoxicity. *J Pharm Pharmacol* 2007; **59**: 863–870.
6. Tohda C, Hashimoto I, Kuboyama T, Komatsu K. Metabolite 1 of protopanaxadiol-type saponins, an axonal regenerative factor, stimulates teneurin-2 linked by PI3-kinase cascade. *Neuropsychopharmacology* 2006; **31**: 1158–1164.
7. Park MJ, Bae CS, Lim SK, Kim DI, Lim JC, Kim JC *et al.* Effect of protopanaxadiol derivatives in high glucose-induced fibronectin expression in primary cultured rat mesangial cells: role of mitogen-activated protein kinases and Akt. *Arch Pharm Res* 2010; **33**: 151–157.
8. Hanzal-Bayer MF, Hancock JF. Lipid rafts and membrane traffic. *FEBS Lett* 2007; **581**: 2098–2104.
9. Lingwood D, Simons K. Lipid rafts as a membrane-organizing principle. *Science* 2010; **327**: 46–50.
10. de Almeida RF, Loura LM, Prieto M. Membrane lipid domains and rafts: current applications of fluorescence lifetime spectroscopy and imaging. *Chem Phys Lipids* 2009; **157**: 61–77.
11. Yi JS, Choo HJ, Cho BR, Kim HM, Kim YN, Ham YM *et al.* Ginsenoside Rh2 induces ligand-independent Fas activation via lipid raft disruption. *Biochem Biophys Res Commun* 2009; **385**: 154–159.
12. Garcia A, Cayla X, Fleischer A, Guergnon J, Alvarez-Franco Canas F, Rebollo MP *et al.* Rafts: a simple way to control apoptosis by subcellular redistribution. *Biochimie* 2003; **85**: 727–731.
13. Dufour C, Guenou H, Kaabeche K, Bouvard D, Sanjay A, Marie PJ. FGFR2-Cbl interaction in lipid rafts triggers attenuation of PI3K/Akt signaling and osteoblast survival. *Bone* 2008; **42**: 1032–1039.
14. Gao X, Zhang J. Akt signaling dynamics in plasma membrane microdomains visualized by FRET-based reporters. *Commun Integr Biol* 2009; **2**: 32–34.
15. Lasserre R, Guo XJ, Conchonaud F, Hamon Y, Hawchar O, Bernard AM *et al.* Raft nanodomains contribute to Akt/PKB plasma membrane recruitment and activation. *Nat Chem Biol* 2008; **4**: 538–547.
16. Matheny Jr RW, Adamo ML. Current perspectives on Akt Akt-ivation and Akt-ions. *Exp Biol Med (Maywood)* 2009; **234**: 1264–1270.
17. Osaki M, Oshimura M, Ito H. PI3K-Akt pathway: its functions and alterations in human cancer. *Apoptosis* 2004; **9**: 667–676.
18. Ayllon V, Fleischer A, Cayla X, Garcia A, Rebollo A. Segregation of Bad from lipid rafts is implicated in the induction of apoptosis. *J Immunol* 2002; **168**: 3387–3393.
19. Datta SR, Dudek H, Tao X, Masters S, Fu H, Gotoh Y *et al.* Akt phosphorylation of BAD couples survival signals to the cell-intrinsic death machinery. *Cell* 1997; **91**: 231–241.
20. del Peso L, Gonzalez-Garcia M, Page C, Herrera R, Nunez G. Interleukin-3-induced phosphorylation of BAD through the protein kinase Akt. *Science* 1997; **278**: 687–689.
21. Adam RM, Mukhopadhyay NK, Kim J, Di Vizio D, Cinar B, Boucher K *et al.* Cholesterol sensitivity of endogenous and myristoylated Akt. *Cancer Res* 2007; **67**: 6238–6246.
22. Gao X, Zhang J. Spatiotemporal analysis of differential Akt regulation in plasma membrane microdomains. *Mol Biol Cell* 2008; **19**: 4366–4373.
23. Arcaro A, Aubert M, Espinosa del Hierro ME, Khanzada UK, Angelidou S, Tetley TD *et al.* Critical role for lipid raft-associated Src kinases in activation of PI3K-Akt signalling. *Cell Signal* 2007; **19**: 1081–1092.
24. Kwon HY, Kim EH, Kim SW, Kim SN, Park JD, Rhee DK. Selective toxicity of ginsenoside Rg3 on multidrug resistant cells by membrane fluidity modulation. *Arch Pharm Res* 2008; **31**: 171–177.
25. Olmsted JB, Carlson K, Klebe R, Ruddle F, Rosenbaum J. Isolation of microtubule protein from cultured mouse neuroblastoma cells. *Proc Natl Acad Sci USA* 1970; **65**: 129–136.
26. Clark MJ, Homer N, O'Connor BD, Chen Z, Eskin A, Lee H *et al.* U87MG decoded: the genomic sequence of a cytogenetically aberrant human cancer cell line. *PLoS Genet* 2010; **6**: e1000832.
27. Raghu H, Sodadasu PK, Malla RR, Gondi CS, Estes N, Rao JS. Localization of uPAR and MMP-9 in lipid rafts is critical for migration, invasion and angiogenesis in human breast cancer cells. *BMC Cancer* 2010; **10**: 647.
28. Mendoza MC, Blenis J. PHLPPing it off: phosphatases get in the Akt. *Mol Cell* 2007; **25**: 798–800.
29. Dibble CC, Manning BD. A molecular link between AKT regulation and chemotherapeutic response. *Cancer Cell* 2009; **16**: 178–180.
30. Pei H, Li L, Fridley BL, Jenkins GD, Kalari KR, Lingle W *et al.* FKBP51 affects cancer cell response to chemotherapy by negatively regulating Akt. *Cancer Cell* 2009; **16**: 259–266.
31. Gao T, Furnari F, Newton AC. PHLPP: a phosphatase that directly dephosphorylates Akt, promotes apoptosis, and suppresses tumor growth. *Mol Cell* 2005; **18**: 13–24.
32. Brognard J, Newton AC. PHLiPPing the switch on Akt and protein kinase C signaling. *Trends Endocrinol Metab* 2008; **19**: 223–230.
33. Brognard J, Sierecki E, Gao T, Newton AC. PHLPP and a second isoform PHLPP2, differentially attenuate the amplitude of Akt signaling by regulating distinct Akt isoforms. *Mol Cell* 2007; **25**: 917–931.
34. Chin YR, Toker A. Function of Akt/PKB signaling to cell motility, invasion and the tumor stroma in cancer. *Cell Signal* 2009; **21**: 470–476.
35. Liang CC, Park AY, Guan JL. *In vitro* scratch assay: a convenient and inexpensive method for analysis of cell migration *in vitro*. *Nat Protoc* 2007; **2**: 329–333.
36. Attele AS, Wu JA, Yuan CS. Ginseng pharmacology: multiple constituents and multiple actions. *Biochem Pharmacol* 1999; **58**: 1685–1693.
37. Bozulic L, Hemmings BA. PIKKing on PKB: regulation of PKB activity by phosphorylation. *Curr Opin Cell Biol* 2009; **21**: 256–261.
38. Li N, Shaw AR, Zhang N, Mak A, Li L. Lipid raft proteomics: analysis of in-solution digest of sodium dodecyl sulfate-solubilized lipid raft proteins by liquid chromatography-matrix-assisted laser desorption/ionization tandem mass spectrometry. *Proteomics* 2004; **4**: 3156–3166.
39. Taghibiglou C, Bradley CA, Gaertner T, Li Y, Wang Y, Wang YT. Mechanisms involved in cholesterol-induced neuronal insulin resistance. *Neuropharmacology* 2009; **57**: 268–276.
40. Yue PY, Leung EP, Mak NK, Wong RN. A simplified method for quantifying cell migration/wound healing in 96-well plates. *J Biomol Screen* 2010; **15**: 427–433.